A Model and Experimental Study of Evaporation from Bare-Soil Surfaces

JUNSEI KONDO AND NOBUKO SAIGUSA

Geophysical Institute, Tohoku University, Sendai, Japan

TAKESHI SATO

Shinjo Branch of Snow and Ice Studies, National Research Institute for Earth Science and Disaster Prevention, Shinjo, Japan

(Manuscript received 22 April 1991, in final form 2 August 1991)

ABSTRACT

A model is constructed for estimating evaporation from bare-soil surfaces. In the model, the evaporation is parameterized with the soil-water content for the upper 2 cm of the soil (Kondo et al.), and the heat and water transport within the soil layer below 2 cm is explicitly described by the heat conduction and moisture diffusion equations.

Experiments on evaporation from loam packed in pans are also carried out. The present model well simulates the observed evaporation and vertical profiles of soil temperature and water content.

Long time simulations of evaporation by the present model are compared with the force–restore method and the bucket model for a drying period of over several months. The decrease in evaporation rate for the bucket model is comparatively small. However, the evaporation by the present model and the force–restore method decreases rapidly several days after the beginning of the drying period. Differences between the evaporation by the present model and that by the force–restore method appear after approximately 10 days from the onset of the drying period.

The sensitivity of the present model on the wind velocity is tested. The evaporation is sensitive to the wind velocity when the soil is wet, but less sensitive when the soil is dried because the soil resistance to the water transport becomes large as compared with the aerodynamical resistance.

1. Introduction

The heat and water exchange between air and land surfaces are two of the important processes of the earth's energy budget and hydrologic cycle. The evaporation from bare soils—a basic process of land hydrology—is greatly affected by soil moisture as well as the condition of the overlying air.

Two problems exist for the estimation of evaporation from bare-soil surfaces: the evaporation mechanism is affected by both atmospheric and soil-moisture properties near the ground surfaces. Also, the water transport in the soil is not well defined.

Philip (1957) suggested detailed equations that describe the heat and water transport in the soil. Sasamori (1970), McCumber and Pielke (1981), and Camillo et al. (1983) developed soil models based on Philip's equations and included them in atmospheric boundary-layer models. Using these soil–atmosphere models, they examined the influence of soil hydrology on the surface energy budget and boundary-layer development.

Deardorff (1978) applied the force–restore method to achieve a surface soil-moisture forecast. The force–restore method (FRM) had originally been developed for a simple prediction of land surface temperatures. Toya and Yasuda (1988) succeeded in simulating surface soil-water content and evaporation by the FRM. The method easily predicts the evaporation, but is somewhat empirical. Further investigation is required for the practical use under various soil and atmospheric conditions.

The hydrologic cycle of most current general circulation and numerical prediction models are mainly based on the so-called "bucket model" (for example, see Manabe 1969 and Hansen et al. 1983).

Several empirical methods have been proposed in soil models to express the evaporation based on surface soil-water content. Recently, Kondo et al. (1990) suggested a new parameterization scheme that related the evaporation to the averaged soil-water content of a 2-cm soil surface layer, which considered the water vapor transport from soil pores in the soil surface layer to the atmosphere.

This study presents a soil model in which the parameterization of the evaporation by Kondo et al. (1990) is included. In the present model, the water and heat transport within the soil are calculated according to Philip (1957). The model and boundary conditions are discussed in sections 2 and 3, respectively. The outdoor experiments performed to test the model are dis-

Corresponding author address: Professor Junsei Kondo, Geophysical Institute, Tohoku University, Sendai 980, Japan.

cussed in section 4. In section 5 the present model is compared with other current soil models such as the force–restore method and the bucket model, to examine the difference in model response during a drying period of over several months. At last, the sensitivity of the present model on the wind velocity is discussed.

2. Soil model

Heat and water transport within the soil is expressed by the heat conduction and moisture diffusion equations. These are fundamentally based on the equations given by Philip (1957). The rates of soil water and temperature change are expressed as

$$\frac{\partial \theta}{\partial t} = -\frac{1}{\rho_w}\frac{\partial q_\theta}{\partial z} \tag{1}$$

and

$$\frac{\partial T}{\partial t} = -\frac{1}{C}\frac{\partial q_h}{\partial z}, \tag{2}$$

where θ is the volumetric soil-water content, t the time, ρ_w the liquid water density, q_θ the moisture flux, z the depth, T the soil temperature, C the volumetric heat capacity, and q_h the heat flux.

The variables q_θ and q_h are given by

$$q_\theta = q_{\theta,\mathrm{liq}} + q_{\theta,\mathrm{vap}}, \tag{3}$$

$$q_h = -\lambda_0 \frac{\partial T}{\partial z} + l q_{\theta,\mathrm{vap}}, \tag{4}$$

where $q_{\theta,\mathrm{liq}}$ is the liquid water flux, $q_{\theta,\mathrm{vap}}$ the water vapor flux in the soil, λ_0 the thermal conductivity of the soil, and l the latent heat of vaporization. Equation (3) describes the moisture flux in the soil as a sum of the liquid water flux and the water vapor flux. Equation (4) shows that the heat flux consists of a heat conduction term and latent heat flux resulting from the water vapor flux.

The liquid water flux $q_{\theta,\mathrm{liq}}$ can be further expressed as

$$q_{\theta,\mathrm{liq}} = -\rho_w D_{\theta,\mathrm{liq}}\frac{\partial \theta}{\partial z} - \rho_w D_{T,\mathrm{liq}}\frac{\partial T}{\partial z} - \rho_w K. \tag{5}$$

Here $D_{\theta,\mathrm{liq}}$ and $D_{T,\mathrm{liq}}$ are diffusion coefficients for liquid water given by

$$D_{\theta,\mathrm{liq}} \equiv K\frac{\partial \psi}{\partial \theta} \tag{6}$$

and

$$D_{T,\mathrm{liq}} \equiv K\frac{\partial \psi}{\partial T}, \tag{7}$$

where K is the hydraulic conductivity and ψ the matric potential.

The water vapor flux $q_{\theta,\mathrm{vap}}$ can be expressed by a tortuosity and porosity factor $f(\theta)$ and the water vapor density in a soil pore ρ_v as

$$q_{\theta,\mathrm{vap}} = -D_{\mathrm{atm}} f(\theta)\frac{\partial \rho_v}{\partial z}, \tag{8}$$

where D_{atm} is the diffusion coefficient for water vapor in the air.

The relative humidity in the soil pore h_θ is defined as

$$h_\theta = \frac{\rho_v}{\rho_0}, \tag{9}$$

where ρ_0 is the saturation density of the water vapor. The humidity of the air adjacent to the water in the soil is determined through the thermodynamical relationship as follows (Philip 1957), and this humidity is often assumed to be equal to h_θ. The humidity can also be written as

$$h_\theta = \exp\left(\frac{\psi g}{RT}\right), \tag{10}$$

where g is the acceleration of gravity and R is the gas constant for water vapor. However, in a previous paper (Kondo et al. 1990) it was suggested that Eq. (10) is invalid near the surface of a natural soil. This is because Eq. (10) is only applicable if an equilibrium between liquid water and the vapor in the soil pores is maintained. During the drying period, however, vapor in the large pores is successively transported to the atmosphere, so the vapor density in the soil pore is not in equilibrium with the averaged soil-water content at that depth.

Based on Fig. 4 of Kondo et al. (1990), h_θ was experimentally obtained as

$$h_\theta = \min\left(1, \frac{\theta}{\theta_H}\right), \quad (0 \leqslant \theta \leqslant \theta_{\mathrm{sat}}) \tag{11}$$

where θ_{sat} is the soil-water content at saturation, and θ_H is the water content that depends on soil type. When the water content is below θ_H, the water vapor in the soil pore is considered not to be saturated. Water content $\theta_H = 0.15$ is assumed for loam used in this study. Equation (11) states that the humidity of the air in the soil pore roughly takes a value midway between the humidity of the air adjacent to the water in the soil pore and that at the ground roughness height z_q. The humidity at z_q was discussed in Kondo et al. (1990).

The flux of water vapor $q_{\theta,\mathrm{vap}}$ is rewritten, making use of Eqs. (8) and (9) as

$$\begin{aligned} q_{\theta,\mathrm{vap}} &= -D_{\mathrm{atm}} f(\theta)\rho_0\frac{\partial h_\theta}{\partial z} - D_{\mathrm{atm}} f(\theta) h_\theta \frac{\partial \rho_0}{\partial z} \\ &= -\rho_w D_{\theta,\mathrm{vap}}\frac{\partial \theta}{\partial z} - \rho_w D_{T,\mathrm{vap}}\frac{\partial T}{\partial z}, \end{aligned} \tag{12}$$

where $D_{\theta,\mathrm{vap}}$ and $D_{T,\mathrm{vap}}$ are the diffusion coefficients for water vapor and are given by

$$\rho_w D_{\theta,\mathrm{vap}} \equiv D_{\mathrm{atm}} f(\theta)\rho_0\frac{\partial h_\theta}{\partial \theta}, \tag{13}$$

$$\rho_w D_{T,\text{vap}} \equiv D_{\text{atm}} f(\theta) h_\theta \frac{\partial \rho_0}{\partial T}. \quad (14)$$

Rewriting q_θ and q_h with use of Eqs. (3), (4), (5), and (12) results in

$$q_\theta = -\rho_w D_\theta \frac{\partial \theta}{\partial z} - \rho_w D_T \frac{\partial T}{\partial z} - \rho_w K, \quad (15)$$

$$q_h = -\lambda \frac{\partial T}{\partial z} + l\rho_w D_{\theta,\text{vap}} \frac{\partial \theta}{\partial z}, \quad (16)$$

where

$$D_\theta = D_{\theta,\text{liq}} + D_{\theta,\text{vap}}, \quad (17)$$

$$D_T = D_{T,\text{liq}} + D_{T,\text{vap}}, \quad (18)$$

and

$$\lambda = \lambda_0 + l\rho_w D_{T,\text{vap}}. \quad (19)$$

Here λ is the modified thermal conductivity.

Some soil parameters can be given as functions of the soil-water content θ. According to Clapp and Hornberger (1978), the matric potential ψ and hydraulic conductivity K can be expressed as

$$\psi(\theta) = \psi_{\text{sat}} \left(\frac{\theta}{\theta_{\text{sat}}} \right)^{-b}, \quad (20)$$

$$K(\theta) = K_{\text{sat}} \left(\frac{\theta}{\theta_{\text{sat}}} \right)^{2b+3}, \quad (21)$$

where ψ_{sat} and K_{sat} are the matric potential and hydraulic conductivity at saturation, while the constant b depends on soil type. For the loam used in the present study, ψ_{sat}, K_{sat}, b, and θ_{sat} are found to be -0.478 m, 6.96×10^{-6} m s^{-1}, 5.39, and 0.49, respectively.

The porosity and tortuosity factor $f(\theta)$ determines the reduction of the volume of pores available for vapor diffusion by soil particles and liquid water. The factor $f(\theta)$ has been expressed by Jackson et al. (1974) as

$$f(\theta) = 0.66(\theta_{\text{sat}} - \theta). \quad (22)$$

The saturation vapor density ρ_0 (kg m^{-3}) is a function of temperature, having been given by Kimball et al. (1976) as

$$\rho_0 = 10^3 \times \exp\left(R_0 - \frac{R_1}{T} \right), \quad (23)$$

where R_0 is 6.0035, and R_1 is 4975.9 K.

The modified thermal conductivity of the soil λ normally depends on the soil-water content; that is, the wet soil has larger value of λ. However, a constant value of $\lambda = 0.2514$ J m^{-1} s^{-1} K^{-1} is used in the present study. The evaporation calculated by the present model is not so sensitive to λ. For example, if λ is increased twice, the amplitude of soil temperature at about 0–10 cm in depth becomes several degrees larger, but evaporation rate hardly changes.

The volumetric heat capacity C is expressed as

$$C = (1 - \theta_{\text{sat}}) C_{\text{soil}} + \theta C_{\text{water}} \quad (24)$$

where C_{soil} and C_{water} are the heat capacity of the soil particles and that of water, respectively. Here $C_{\text{soil}} = 1.26 \times 10^6$ J m^{-3} K^{-1} and $C_{\text{water}} = 4.20 \times 10^6$ J m^{-3} K^{-1} are used as typical values. The heat capacity of air is omitted, since it is small when compared with that of the other constituents of the soil.

The equations for heat and water transport introduced in this section are transformed to the finite-difference equations and solved by forward-difference scheme.

3. Boundary conditions

Boundary conditions are required at the surface and bottom of the soil layer for both moisture and temperature.

The energy balance equation at the soil surface is expressed as

$$R^\downarrow = \sigma T_s^4 + H + lE + G, \quad (25)$$

where $R^\downarrow$ is the incoming radiation, σ the Stefan–Boltzmann constant, σT_s^4 the longwave radiation from the soil surface, H the sensible heat flux, lE the latent heat flux, and G the heat flux into the soil. Each energy component can be written as

$$R^\downarrow = (1 - a) S^\downarrow + L^\downarrow, \quad (26)$$

$$H = c_p \rho C_H u (T_s - T_a), \quad (27)$$

$$lE = l\rho C_E u [q^*(T_s) - q_a][1 + C_E u F(\theta)/D_{\text{atm}}]^{-1}, \quad (28)$$

$$G = -\lambda \left(\frac{\partial T}{\partial z} \right)_{z=0}, \quad (29)$$

where a is the albedo of the soil, $S^\downarrow$ the solar radiation, $L^\downarrow$ the atmospheric radiation, c_p the specific heat of air, ρ the air density, C_H the bulk coefficient for the sensible heat flux, u the wind speed, T_s the soil surface temperature, and T_a the air temperature.

The parameterization of evaporation shown in Eq. (28) was developed by Kondo et al. (1990), where E is the rate of evaporation, C_E the bulk coefficient for the water vapor flux, $q^*(T_s)$ the saturated specific humidity at the surface temperature T_s, q_a the specific humidity of the air, and $F(\theta)$ the resistance of the soil pores in the surface soil layer (2 cm thick) to the transport of water vapor.

Here $F(\theta)$ should be found experimentally for every soil type. The value of $F(\theta)$ was determined from Eq. (28) using the observed values of E, u, T_s, q_a, and θ. According to Kondo et al. (1990), $F(\theta)$ is regarded to be a function of the averaged soil-water content of the 2-cm surface layer and expressed as

$$F(\theta) = \begin{cases} F_1(\theta_{\text{sat}} - \theta)^{F_2} & [q^*(T_s) > q_a] \\ 0 & [q^*(T_s) < q_a] \end{cases} \quad (30)$$

Table 1 shows the constants F_1, F_2, and θ_{sat} for various soil type.

It should be noted that the thickness of 2 cm was determined for convenience. If the soil layer is thicker than 2 cm, then $F(\theta)$ is larger than the value calculated by Eq. (30), and if it is thinner than 2 cm, $F(\theta)$ is smaller, because θ almost always increases with depth during a drying period. To calculate the evaporation, the surface layer should be chosen as thin as possible so as to be sensitive to the change of surface water content, but too thin a layer has difficulty in comparing with the observation. Rather, a thinner depth than 2 cm may be adequate for a case of a fast drying surface such as a sand field.

According to the situation, different boundary conditions can be considered at the bottom of the soil layer. For example, if the soil temperature and moisture do not change at the bottom, the boundary conditions

$$\left(\frac{\partial q_\theta}{\partial z}\right)_{z=z_n} = 0, \tag{31}$$

and

$$\left(\frac{\partial q_h}{\partial z}\right)_{z=z_n} = 0 \tag{32}$$

are suitable, where z_n is the soil-layer depth in the model.

If the heat and moisture fluxes at z_n are equal to zero,

$$q_\theta = 0, \quad q_h = 0 \quad \text{at } z = z_n, \tag{33}$$

can be used. If drainage through the bottom boundary exists, the boundary condition for the moisture flux is given as

$$q_\theta = -\rho_w K(\theta) \quad \text{at } z = z_n. \tag{34}$$

4. Pan experiments and model calculations

The soil model was constructed in the previous section using a parameter $F(\theta)$ decided empirically. In this section, two experiments were performed under different soil-moisture conditions (Table 2), and results were compared with model calculations under experimental conditions. The purpose of these experiments and simulations is to develop the model that is available for the long time simulation, and to compare with models used recently for the numerical weather prediction or the climate researches.

Uniformly wet soil, made by mixing water and dry soil, was packed in a pan with a diameter of 30 cm. The time variation of soil temperature, water content, and evaporation from the soil were observed outdoors over a period of several days.

TABLE 1. Constants of $F(\theta)$.

Soil type	F_1 (m)	F_2	θ_{sat}
Loam	2.16×10^2	10.0	0.490
Sand	8.32×10^5	16.6	0.392
Fine sand	7.00×10^3	11.2	0.397

TABLE 2. Summary of the two experiments.

	Experiment 1	Experiment 2
Period	6–8 June 1988	30 May–5 June 1989
Initial θ*	0.100	0.236
Soil layer (cm)	0–13	0–10
Soil temperature (cm)	1, 3, 7, 13	1, 3, 5.5, 8.5

* Initial value of volumetric soil-water content.

Figure 1 displays the circular pan used in the present experiment. The hourly averaged evaporation rate (latent heat) was obtained by weighing the soil every hour, with errors of less than 0.01 mm h^{-1} (7 W m^{-2}).

The observed elements are solar radiation, atmospheric radiation, air temperature, specific humidity, wind velocity at a height of 50 cm above the soil, the surface temperature of the soil, and temperatures at four levels within the soil. The weather condition during the experiments was generally clear with scattered clouds.

In the model calculations, the observed profile of soil temperature at the beginning of the experiment was used as the initial conditions. The model soil was divided into four layers, and the equations were integrated with a time step of 5 min. Hourly averaged solar radiation, atmospheric radiation, air temperature, specific humidity, and wind velocity are used as the external conditions in the model calculations.

In this study, bulk coefficients C_H and C_E are assumed to be equal. Generally, C_E for a horizontal surface depends on the surface roughness and atmospheric stability. The coefficient C_E for a limited small surface, depends additionally on the Reynolds number Re based on the scale of the surface. The value of C_E for the present experiments was determined from Eq. (28)

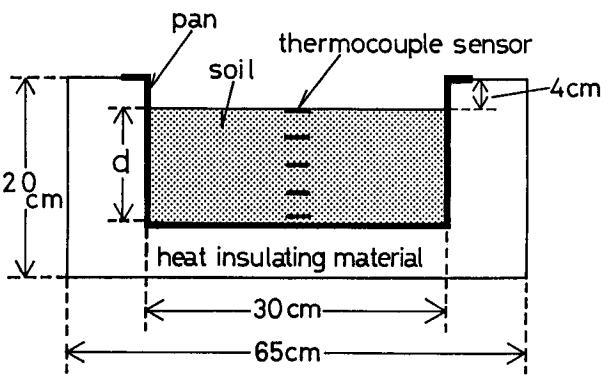

FIG. 1. Illustration of the soil packed in the experimental circular pan. The letter d represents the soil depth, equal to 13 cm in experiment 1, and 10 cm in experiment 2.

by measuring the soil surface temperature and the evaporation from a fully wet soil in another pan with the same structure as used presently. It should be noted that $F(\theta)$ is zero when the surface is sufficiently wet.

According to the theoretical and semiempirical expression of water-transport coefficient for the limited surface, C_E for the present experiments is expressed as

$$C_E = 1.26\mathrm{Sc}^{-2/3}\mathrm{Re}^{-1/2}, \quad (5.7 \times 10^3 < \mathrm{Re} < 4.2 \times 10^4) \qquad (35)$$

where

$$\mathrm{Sc} = \frac{\nu}{D_{\mathrm{atm}}},$$

and

$$\mathrm{Re} = \frac{xu}{\nu}.$$

Also, Sc is the Schmidt number, ν the kinematic viscosity of air, and x the pan size (=0.3 m in the present study). Typical value of $C_E u$ during the experiments was 1×10^{-2}–3×10^{-2} m s^{-1}.

A solid line in Fig. 2 shows the observed albedo for loam used in this study, which can be expressed by

$$a = \begin{cases} -0.21\theta + 0.24 & (0 \leqslant \theta < 0.14) \\ -1.00\theta + 0.35 & (0.14 \leqslant \theta < 0.22) \\ 0.13 & (0.22 \leqslant \theta < \theta_{\mathrm{sat}}), \end{cases} \qquad (36)$$

where θ is the averaged soil-water content of the 2-cm surface layer ($\theta_{\mathrm{sat}} = 0.49$). A broken line in Fig. 2 is the observed albedo by Idso et al. (1975).

The heat and moisture fluxes at the bottom are set to zero in the calculations.

Figures 3a and 3b are the observed and calculated soil temperatures for experiment 1. Figures 4a and 4b are the same as in Fig. 3, except for experiment 2. In Fig. 4b, the amplitudes of the soil temperature at depths of 3 and 8.5 cm are smaller than those observed (Fig. 4a). This may be due to the underestimation of thermal conductivity for the rather wet soil.

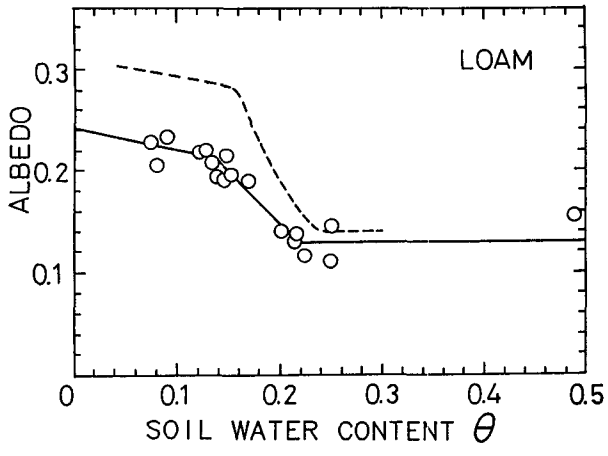

FIG. 2. The observed soil albedo for loam (open circles) versus the surface soil-water content. The solid line represents Eq. (36). The broken line is the observed albedo by Idso et al. (1975).

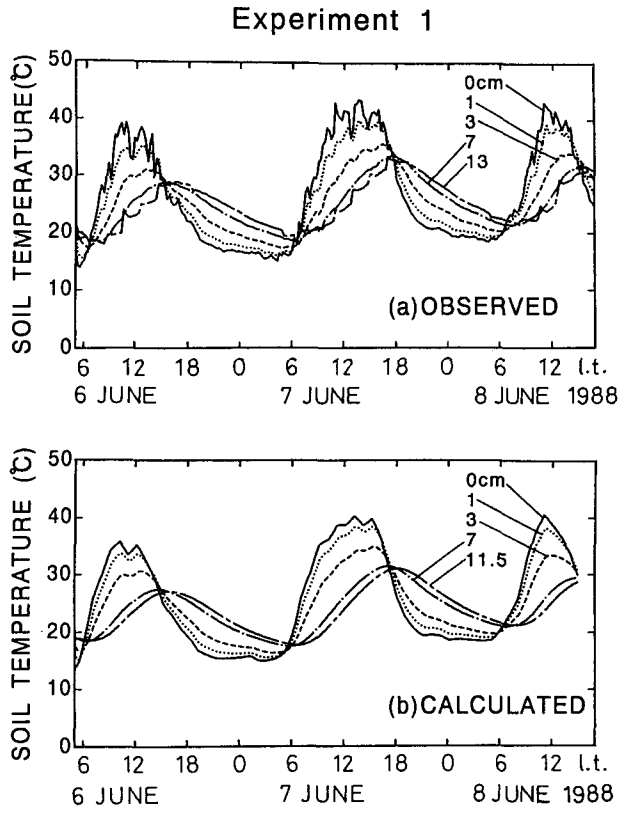

FIG. 3. The temporal variation of soil temperature in experiment 1: (a) observed, (b) calculated.

Figures 5 and 6 show the observed (denoted by symbols) and calculated (solid lines) soil-water content profiles, where the broken line represents the initial profile. The soil-water content at each depth was obtained by an oven drying method. Therefore, the soil-water content profile was only observed once for each pan, since the soil layer is disturbed by the soil sampling. In experiment 2, several similar pans were used and the soil was sampled for each.

Figures 7 and 8 display the time variation of the evaporation (latent heat flux) from the soil for experiments 1 and 2, respectively. Here the solid circles denote the observed values while the solid lines represent those calculated. As can be seen in the figures, the calculated values agree well with those observed.

5. Comparison with other soil models

In this section, the present soil model is compared with two other current models of land hydrology. These are the force–restore method (FRM) proposed by Deardorff (1978) and the bucket model based on

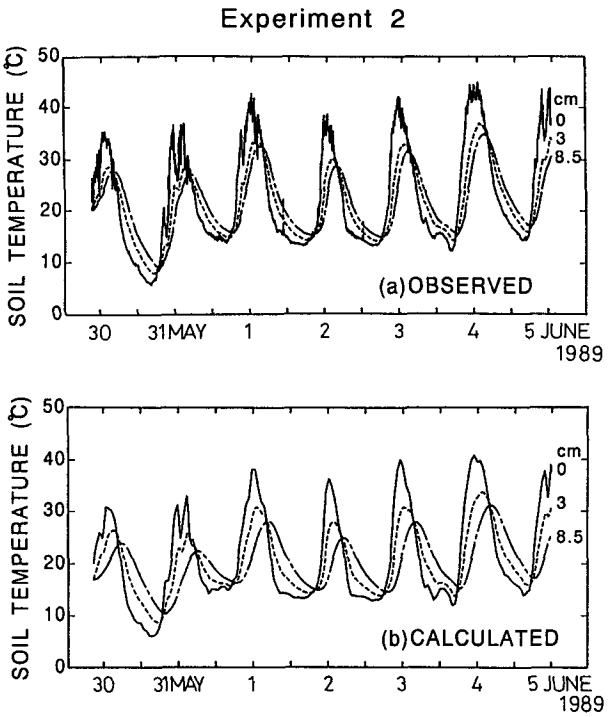

FIG. 4. The same as Fig. 3, except for experiment 2.

Manabe (1969). The model runs were integrated for 187 model days to investigate long-term variations in hydrology.

The external conditions, corresponding to an early summer day at midlatitude, and no precipitation are

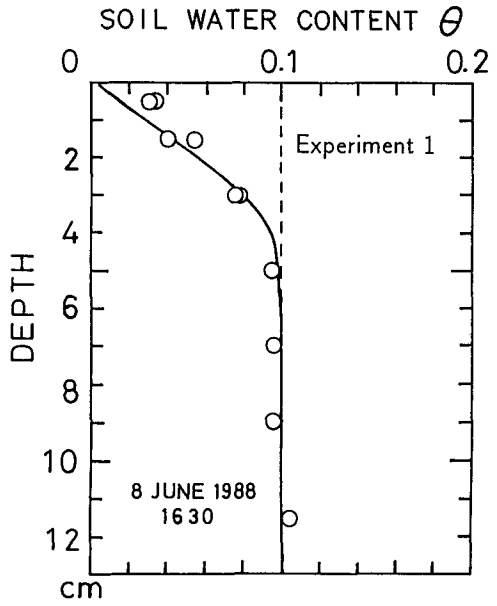

FIG. 5. Soil-water content profiles for experiment 1. The open circles denote observed values, the solid line calculated values, while the broken line is the initial profile.

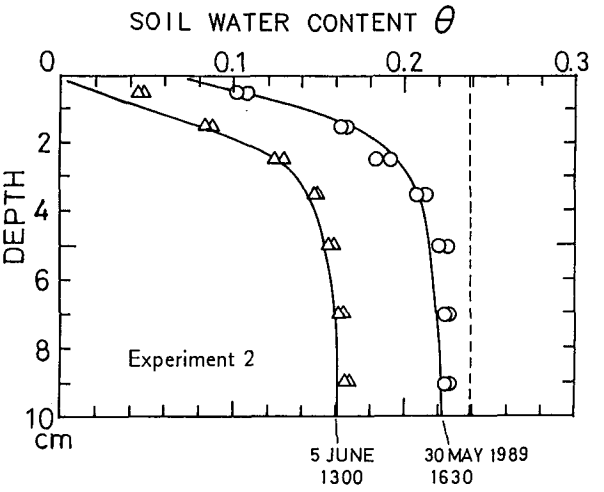

FIG. 6. Same as Fig. 5, except for experiment 2, with open circles denoting observed values for 1630 JST 30 May and the open triangles those on 1300 JST 5 June.

the same for the three models (Table 3). Atmospheric radiation, specific humidity, and the wind velocity are fixed, but solar radiation and air temperature have typical diurnal variations. The initial soil conditions are given as follows. The soil temperature is equal to the mean air temperature, while the soil water is equal to its saturated water content. The bulk coefficients for the sensible and latent heat fluxes, C_H and C_E, are specified as 3.0×10^{-3}, where the reference height is 1.5 m. This value is suitable for rather smooth extensive soil surfaces. The value of $C_E u$ is 1.2×10^{-2} m s^{-1}.

a. The present model

Using the model given in section 2, the soil temperature and water content are calculated at 25 vertical levels, spaced uniformly from the soil surface to a depth of 50 cm. At the bottom boundary, the heat flux is set to zero and the moisture flux is equal to the soil hydraulic coefficient at that depth [from Eq. (34)].

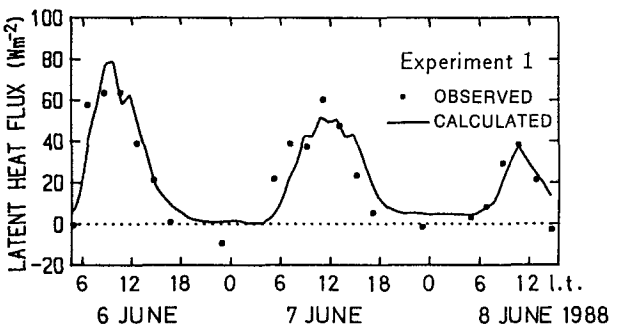

FIG. 7. Temporal variations of the evaporation rate in experiment 1. Solid circles represent observed values, while the solid line is the calculated results.

b. *The force–restore method*

The FRM predicts the "surface" soil-water content θ_s and the "reservoir" water content θ_b as

$$\frac{\partial \theta_s}{\partial t} = -\frac{C_1(E-P)}{\rho_w d_1} - \frac{C_2(\theta_s - \theta_b)}{\tau}, \quad (37)$$

$$\frac{\partial \theta_b}{\partial t} = -\frac{E-P}{\rho_w d_2}, \quad (38)$$

where θ_b is the soil-water content averaged over the depths 0–50 cm, E the evaporation, and P the precipitation. At the depth d_1 (=10 cm) diurnal variation of moisture vanishes, and d_2 (=50 cm) is the depth below which moisture transport is ignored. The time interval τ is taken as 1 day.

According to Deardorff (1978), C_1 and C_2 are given as

$$C_1 = \begin{cases} 0.5 & \left(0.75 \leqslant \dfrac{\theta_s}{\theta_{\text{sat}}}\right) \\ 14 - 22.5\left(\dfrac{\theta_s}{\theta_{\text{sat}}} - 0.15\right) & \left(0.15 \leqslant \dfrac{\theta_s}{\theta_{\text{sat}}} < 0.75\right) \\ 14 & \left(\dfrac{\theta_s}{\theta_{\text{sat}}} < 0.15\right), \end{cases} \quad (39)$$

and

$$C_2 = 0.9. \quad (40)$$

The evaporation rate is written as

$$E = \rho C_E u \beta_F [q^*(T_s) - q_a], \quad (41)$$

and

$$\beta_F = \min\left(1, \frac{\theta_s}{\theta_f}\right), \quad (42)$$

where β_F is the soil surface moisture availability for the FRM, and θ_f equals $0.75\theta_{\text{sat}}$.

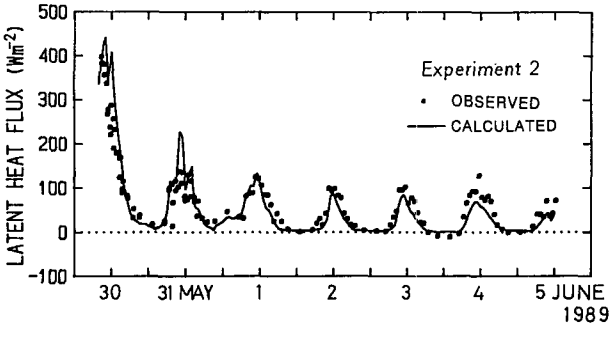

FIG. 8. Same as Fig. 7, except for experiment 2.

TABLE 3. External conditions given for the soil models.

Item	Symbol	Value
Solar radiation	$S^{\downarrow}$	Typical diurnal variation under clear-sky conditions according to Kondo and Miura (1985) (precipitable water is 1.3 cm and atmospheric turbidity is 0.05).
Atmospheric radiation	$L^{\downarrow}$	291 W m^{-2}
Air temperature	T_a	Typical diurnal variation with a daily mean temperature of 13.8°C, and diurnal range of 16°C.
Specific humidity	q_a	6.13×10^{-3}
Wind velocity	u	4 m s^{-1}

c. *The bucket model*

In the bucket model, the time variation of soil water W is given by

$$\frac{\partial W}{\partial t} = -(E' - P'), \quad (43)$$

where E' and P' are the evaporation and precipitation given by

$$E' = \rho C_E u \beta_B [q^*(T_s) - q_a], \quad (44)$$

and

$$\beta_B = \min\left(1, \frac{W}{W_f}\right), \quad (45)$$

respectively. The variable β_B is the moisture availability for the bucket model, and W_f equals $0.75W_{\text{sat}}$, where W_{sat} is the field capacity. Values of W_{sat} equal to 24.5 and 12 cm are adopted in this study.

d. *Comparison*

Figure 9 shows the time variation of the soil-water content for the first 20 days calculated by (a) the present model, (b) the FRM, and (c) the bucket model using W_{sat} = 24.5 cm.

On the first day of the present model (Fig. 9a), the water that cannot be retained by the soil matrix quickly drains into the underlying layer until the soil-water content reaches about $0.73\theta_{\text{sat}}$ at the end of the day. After several days have passed, the average soil-water content of the 0–2-cm layer shows a large amplitude in the diurnal variation due to strong drying over the daytime and moistening by the upward transport of water in the soil layer at night.

Figure 9b for the FRM exhibits two different features from Fig. 9a. First, a rapid decrease in the surface water

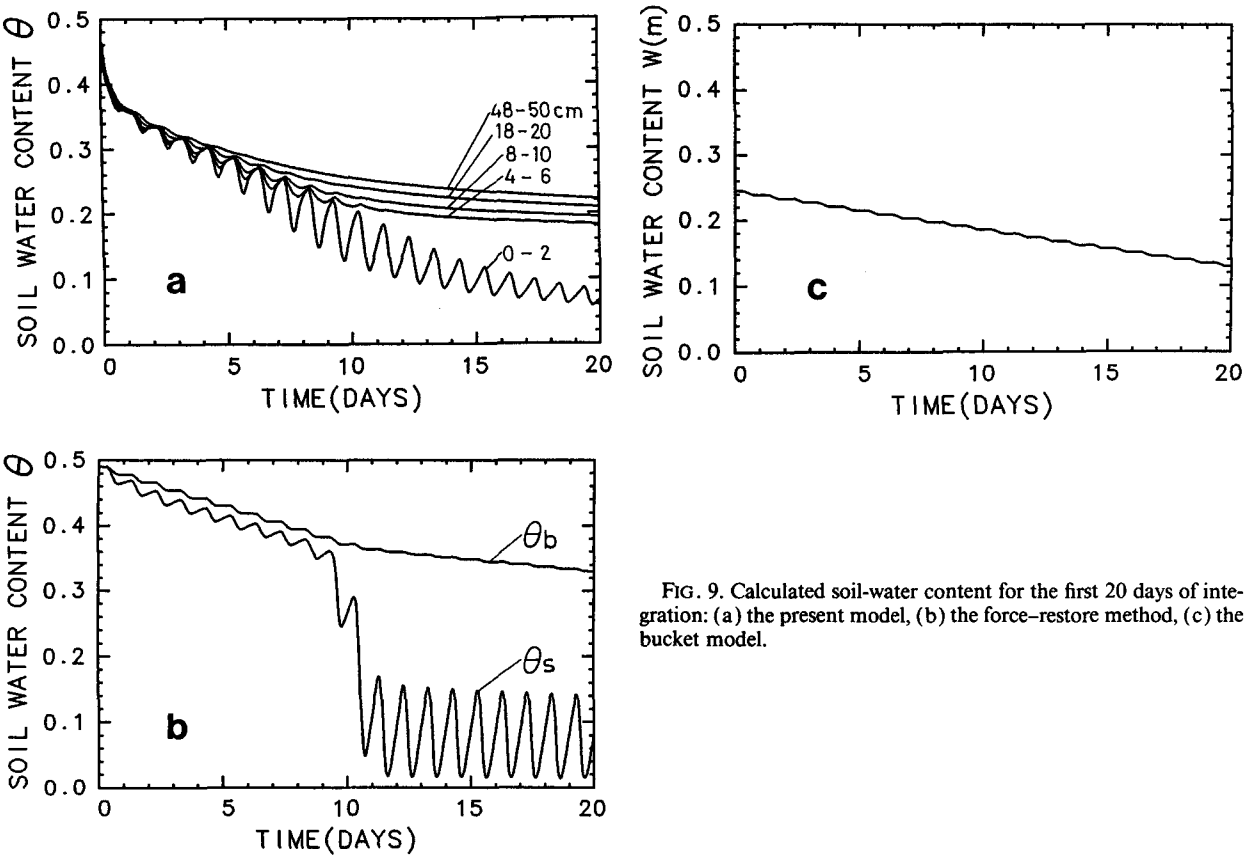

FIG. 9. Calculated soil-water content for the first 20 days of integration: (a) the present model, (b) the force–restore method, (c) the bucket model.

content θ_s does not appear at the onset of the drying, since the FRM does not include drainage process. The second feature is that θ_s reduces suddenly on the tenth day. At this time, the value of C_1 begins to increase in Eq. (39) with decreasing of θ_s. Following Eq. (37), then, θ_s begins to decrease more quickly even if the same evaporation rate continues. The physical meaning of these responses is supposed that the water transport from under the soil layer to surface layer decreases because soil surface layer is strongly dried, then the drying of soil surface layer is accelerated.

In Figure 9c, the soil water W calculated by the bucket model changes slowly, with a rather small diurnal variation when compared with the two other models. This is because the bucket model considers only the soil-water content averaged whole soil layer.

Figure 10 shows the temporal change in the daily averaged latent heat flux by the three soil models. The evaporation [curve (c)] estimated by the bucket model (W_{sat} = 24.5 cm) slowly reduces and vanishes after about 80 days. The curve (c′) is also for the bucket model but uses a value of 12 cm for W_{sat}. The smaller value of W_{sat} causes a sharper decrease in the rate of evaporation, in better agreement with the other models.

On the other hand, the present model [curve (a)] and the FRM [curve (b)] show a very rapid decrease during the first 10–15 days after the onset of the drying period; after which a slight evaporation rate continues for a long period of time. These tendencies depend on the parameterization of the surface evaporation. The bucket model relates the evaporation to the soil-water content averaged for a deep soil layer, while the other two models relate evaporation to the surface soil-water content. Therefore, the latter models can better express

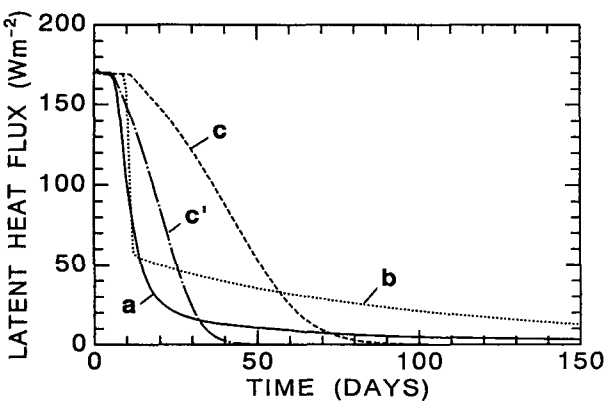

FIG. 10. The temporal change of the daily averaged latent heat flux calculated by curve (a) the present model, curve (b) the force–restore method, curve (c) the bucket model using W_{sat} = 24.5 cm, and curve (c′) the bucket model using W_{sat} = 12 cm.

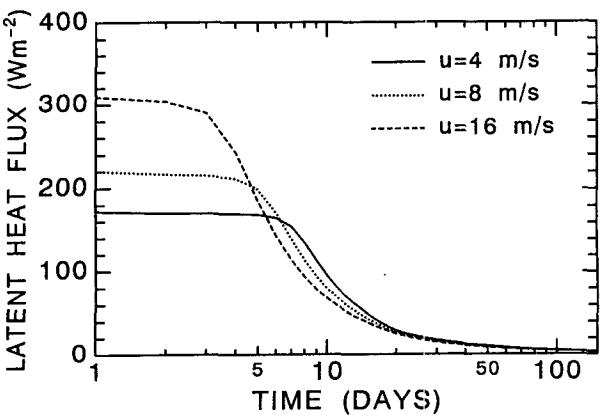

FIG. 11. The daily averaged latent heat flux calculated by the present model. The parameter is u from 4 to 16 m s^{-1}.

the rapid reduction of evaporation caused by the initial drying of the surface soil.

At last, the sensitivity of the present model on the wind velocity u is tested. Figure 11 shows the latent heat flux when u is 4, 8, and 16 m s^{-1}, respectively.

The evaporation rate in the beginning of the drying period is more sensitive to u than that in the latter half of the period. This is because the soil resistance to the water transport is very small when the soil is wet enough, so the rate of evaporation is determined by aerodynamical resistance in the first half of the period.

In the latter half, the soil resistance becomes much larger as compared with the aerodynamical resistance, so the evaporation is determined by the soil hydrological conditions and less sensitive to the wind velocity. The evaporation rate should depend on the soil type in this period.

6. Concluding remarks

A soil model has been described for estimating the evaporation from a bare soil. The model adopts a parameterization scheme for evaporation proposed by Kondo et al. (1990), which considers the water vapor transport process in the surface soil layer. The model also takes into account the diffusion of heat and water within the soil.

Observations of evaporation, soil temperature, and soil-water content were conducted over a period of several days and compared with the model calculations. The observed decrease in the evaporation due to soil drying is well simulated with the present model.

The present model was then compared with the force–restore method and the bucket model. The calculated time variation of evaporation was found to be influenced by the depth of soil layer, whose moisture is related to the evaporation rate in each model. In order to verify the model performance, the observation of evaporation over a longer time interval should be carried out in field experiments.

The sensitivity test of the present model on the wind velocity has been carried out. The evaporation is sensitive to the wind velocity when the soil is wet, because the soil resistance to the water transport is so small that the evaporation is determined, almost by aerodynamical resistance. The evaporation is less sensitive when the soil is dried because the soil resistance becomes larger as compared with the aerodynamical resistance.

This model treats only drying period. If the precipitation exists, the discussion of penetration is needed.

The parameterization using the resistance of the soil to the transport of water $F(\theta)$ was shown to simulate the observed evaporation. Although $F(\theta)$ was determined experimentally, it is necessary to relate the formulation of $F(\theta)$ to the soil structure in order to generalize $F(\theta)$, and to apply it to various soil surfaces. Microscopic water transport in the soil pore is also an important and essential process for the evaporation from bare-soil surfaces. These problems require further theoretical and observational study.

REFERENCES

Camillo, P. J., R. J. Gurney, and T. J. Schmugge, 1983: A soil and atmospheric boundary layer model for evapotranspiration and soil moisture studies. *Water Resour. Res.*, **19**, 371–380.

Clapp, R. B., and G. M. Hornberger, 1978: Empirical equations for some soil hydraulic properties. *Water Resour. Res.*, **14**, 601–604.

Deardorff, J. W., 1978: Efficient prediction of ground surface temperature and moisture, with inclusion of a layer of vegetation. *J. Geophys. Res.*, **83**, 1889–1903.

Hansen, J., G. Russell, D. Rind, P. Stone, A. Lacis, S. Lebedeff, R. Ruedy, and L. Travis, 1983: Efficient three-dimensional global models for climate studies: Models I and II. *Mon. Wea. Rev.*, **111**, 609–662.

Idso, S. B., R. D. Jackson, R. J. Reginato, B. A. Kimball, and F. S. Nakayama, 1975: The dependence of bare soil albedo on soil water content. *J. Appl. Meteor.*, **14**, 109–113.

Jackson, R. D., R. J. Reginato, B. A. Kimball, and F. S. Nakayama, 1974: Diurnal soil-water evaporation: Comparison of measured and calculated soil water fluxes. *Soil Sci. Soc. Am. Proc.*, **38**, 861–866.

Kimball, B. A., R. D. Jackson, F. S. Nakayama, S. B. Idso, and R. J. Reginato, 1976: Soil-heat flux determination: Temperature gradient method with computed thermal conductivities. *Soil Sci. Soc. Am. J.*, **40**, 25–28.

Kondo, J., and A. Miura, 1985: Surface heat budget of the western pacific for May 1979. *J. Meteor. Soc. Japan.*, **63**, 633–646.

——, N. Saigusa, and T. Sato, 1990: A parameterization of evaporation from bare soil surfaces. *J. Appl. Meteor.*, **29**, 383–387.

Manabe, S., 1969: The atmospheric circulation and the hydrology of the earth's surface. *Mon. Wea. Rev.*, **97**, 739–774.

McCumber, M. C., and R. A. Pielke, 1981: Simulation of the effects of surface fluxes of heat and moisture in a mesoscale numerical model. *J. Geophys. Res.*, **86**, 9929–9938.

Philip, J. R., 1957: Evaporation, and moisture and heat fields in the soil. *J. Meteor.*, **14**, 354–366.

Sasamori, T., 1970: A numerical study of atmospheric and soil boundary layers. *J. Atmos. Sci.*, **27**, 1122–1137.

Toya, T., and N. Yasuda, 1988: Parameterization of evaporation from a non-saturated bare surface for application in numerical prediction models. *J. Meteor. Soc. Japan.*, **66**, 729–739.